Theory of orbital excitation and resonant inelastic x-ray scattering in manganites

Sumio Ishihara and Sadamichi Maekawa
Institute for Materials Research, Tohoku University, Sendai 980-8577 Japan
(Received 30 November 1998; revised manuscript received 12 August 1999)

We study theoretically the collective orbital excitation called the orbital wave in the orbital ordered manganites. The dispersion relation of the orbital wave is strongly correlated with the static spin structure through the coupling between spin and orbital degrees of freedom. As a probe to detect the dispersion relation of the orbital wave, we propose possible excitation processes in the resonant inelastic x-ray scattering. The scattering cross section due to the orbital wave is calculated in several types of the orbital and spin structures.

I. INTRODUCTION

It is widely accepted that one of the important ingredients for the colossal magnetoresistance[1–4] (CMR) and various complex phenomena observed in manganites is the orbital degree of freedom. Although the long range orbital order and its implications in the magnetic interaction were discussed a long time ago,[5–7] it has been recognized as a hidden degree of freedom, because the observation technique has been limited.[8] Recently, resonant x-ray scattering sheds light on the subject, that is, by using this method the orbital order in $La_{0.5}Sr_{1.5}MnO_4$ was directly observed.[9] The alternate orbital alignment was confirmed by observation of the superlattice reflection induced by the anisotropy of the atomic scattering factor. This experimental technique was recognized as a powerful probe to detect the orbital order through intensive experimental and theoretical studies.[10–14]

On the other hand, the dynamics of the orbital degree of freedom is still far from our understanding. In orbital ordered insulators, the collective excitation for the orbital degree of freedom was first investigated by Cyrot and Lyon-Caen in the model where the orbital space was assumed to be isotropic.[15] It was termed *orbital wave* in analogy with spin wave. For actual compounds, the present authors calculated the dispersion relation of the orbital wave in the $(3d_{3x^2-r^2},3d_{3y^2-r^2})$-type orbital ordered state with (A)layer-type antiferromagnetic structure in $LaMnO_3$.[16] It is supposed that the orbital excitation affects the thermodynamic, transport, and optical properties[17] as well as the dispersion relations of the spin wave[18] and phonon. As a probe to observe the orbital excitation, Inoue *et al*. theoretically examined Raman scattering[19] where the excitation process is analogous to that in the magnon Raman scattering. In this method, the information of the orbital wave at the Γ point and its density of states are obtained.

In this paper, we study theoretically the orbital wave in orbital ordered manganites. We calculate the dispersion relation of the orbital wave in several spin structures where spins are assumed to be frozen. It is shown that the anisotropic spin structure brings about the gap of the orbital wave. As a probe to observe the orbital wave, we study the resonant inelastic x-ray scattering (RIXS). RIXS is rapidly developed through the recent progress of the synchrotron radiation source[20,21] and is applied to several highly correlated electron systems.[22,23] One of the advantages of this method on the subject is that the wavelength of the x ray is comparable to the lattice constant and the dispersion relation of the orbital wave is detectable. We propose the excitation processes of the orbital wave by RIXS and formulate the cross section of the scattering.

In Sec. II, the dispersion relation of the orbital wave is calculated in the several spin structures. In Sec. III, the excitation processes of the orbital wave by RIXS are proposed and the characteristic properties of the cross section are discussed. Section IV is devoted to summary and discussion.

II. ORBITAL WAVE

In order to calculate the collective excitations in an orbital ordered insulator, we start with the Hamiltonian describing the low energy electronic structure in perovskite manganites. The cubic lattice consisting of Mn ions is considered and two e_g orbitals and a t_{2g} localized spin are introduced in each site. The Coulomb interactions between e_g electrons (U,U',J) and the Hund coupling (J_H) between e_g and t_g spins are considered. Because the Coulomb interactions give the largest energy among the relevant parameters, the Hamiltonian is derived by excluding the doubly occupied e_g states as follows,

$$\tilde{H}_{3d}=H_{e\text{-}e}+H_{e\text{-}t}+H_{t\text{-}t}. \tag{1}$$

The detailed derivation is presented in Ref.16. The first term describes the interaction between nearest neighboring (NN) spins and orbitals in e_g orbitals,

$$H_{e\text{-}e}=-2J_1\sum_{\langle ij\rangle}\left(\frac{3}{4}+\mathbf{S}_i\cdot\mathbf{S}_j\right)\left(\frac{1}{4}-\Psi_i^{\dagger}\tau_{ij}\Psi_j\right)$$
$$-2J_2\sum_{\langle ij\rangle}\left(\frac{1}{4}-\mathbf{S}_i\cdot\mathbf{S}_j\right)\left(\frac{3}{4}+\Psi_i^{\dagger}\tau_{ij}\Psi_j+A_{ij}\right), \tag{2}$$

where a relation $U=U'+J$ is assumed with U, U', and J being the intra- and inter-orbital Coulomb interactions and the exchange interaction in e_g orbitals, respectively. $J_1=t_0^2/(U'-J)$ and $J_2=t_0^2/(U'+J+2J_H)$ with $J_1>J_2$. t_0 is the hopping integral between the nearest neighboring $3d_{3z^2-r^2}$ orbitals in the z direction. $\Psi_i=[T_{iz},T_{ix}]^t$ is a doublet of the orbital pseudospin operator: $\mathbf{T}_i$

$=(1/2)\Sigma_{\sigma\gamma\gamma'}\tilde{d}^{\dagger}_{i\gamma\sigma}(\boldsymbol{\sigma})_{\gamma\gamma'}\tilde{d}_{i\gamma'\sigma}$ and $\mathbf{S}_i$ is the spin operator with $S=1/2$ for an e_g electron. τ_{ij} and A_{ij} are defined by

$$\tau_{ii+l}=\frac{1}{2}\begin{pmatrix} 1+\cos n_l\frac{2\pi}{3} & \sin n_l\frac{2\pi}{3} \\ \sin n_l\frac{2\pi}{3} & 1-\cos n_l\frac{2\pi}{3} \end{pmatrix}, \tag{3}$$

and

$$A_{ij}=\Psi^{\dagger}_i M_{ij} n_j+\text{H.c.}, \tag{4}$$

respectively, where $M_{ii+l}=(\cos n_l 2\pi/3,-\sin n_l 2\pi/3)^t$ with $(n_x,n_y,n_z)=(1,2,3)$. The forms of τ_{ij} and M_{ij} are obtained by the Slater-Koster formulas for the transfer intensity $t_{ij}^{\gamma\gamma'}$ between site i with orbital γ and site j with γ'. It is worth noting that the orbital part of $H_{e\text{-}e}$ is represented by T_z and T_x, since $t_{ij}^{\gamma\gamma'}$ is rewritten by the rotation matrix of the (T_z,T_x) plane and the projection operator for $3d_{3z^2-r^2}$ orbital. The first term in Eq. (2) favors the ferromagnetic spin structure with the antiferromagnetic-type orbital ordered state where two kinds of orbital sublattice exist. On the other hand, the second one favors the antiferromagnetic structure with the ferromagnetic-type orbital ordered state where the occupied orbital is the same in all sites. The sum of the second and third terms in Eq. (1) is given by

$$H_{e\text{-}t}+H_{t\text{-}t}=-J_H\sum_i \mathbf{S}_{t_{2g}i}\cdot\mathbf{S}_i+J_{AF}\sum_{\langle ij\rangle}\mathbf{S}_{t_{2g}i}\cdot\mathbf{S}_{t_{2g}j}, \tag{5}$$

where $\mathbf{S}_{t_{2g}i}$ is the spin operator for t_{2g} spin with $S=3/2$ and J_{AF} is the antiferromagnetic superexchange interaction between NN t_{2g} spins.

We first study the spin and orbital ordered structures at zero temperature in the mean field approximation. It is assumed that in each Mn site, one of the e_g orbitals is occupied by an electron. For both spin and orbital structures, we introduce four types of the ordered state: ferromagnetic type (F type) where spins or orbitals in all sites are parallel, and three kinds of antiferromagnetic type, that is, layer type (A type), rod type (C type), and NaCl type (G type), where two kinds of spin or orbital sublattice exist. The rotating frame is introduced in the orbital space and the orbital state is described by an angle θ in the (T_z,T_x) plane. In the scheme, the occupied orbital is represented by $|3d_\gamma\rangle=\cos(\theta_\gamma/2)|3d_{3z^2-r^2}\rangle-\sin(\theta_\gamma/2)|3d_{x^2-y^2}\rangle$. As the order parameters, $\langle S_z\rangle$, $\langle S_{t_{2g}z}\rangle$, and $\langle T(\theta)_z\rangle=\cos\theta\langle T_z\rangle-\sin\theta\langle T_x\rangle$ with $\langle S_{t_{2g}z}\rangle=3\langle S_z\rangle$ are introduced.

The mean field phase diagram is presented in Fig. 1. A sequential change in the spin structure, that is, $F\rightarrow A\rightarrow C\rightarrow G$ with increasing J_2 and J_{AF} is caused by an enhancement of the antiferromagnetic interactions. As for the orbital structure in the spin-F and spin-G phases, the orbital-G phase with $(\theta_A,\theta_B)=(\theta_A,\theta_A+\pi)$-type ordered state for any θ_A and the orbital-C phase with a $(\theta_A,\theta_B)=(\pi/2,3\pi/2)$-type state are the mean field solutions.[7,24,25] θ_A and θ_B are the angles in A and B orbital sublattices, respectively. In the orbital-G case, especially, the orbital space becomes isotropic in the (T_z,T_x) plane, although the orbital part in the Hamiltonian [Eq. (2)] is not written by a simple vector product. This result originates from the following two conditions: (1) the relation,

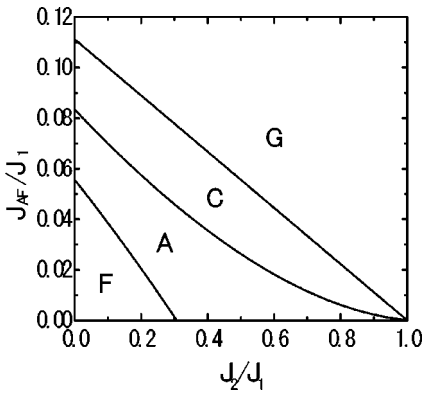

FIG. 1. The mean field phase diagram at zero temperature. F, A, C, and G imply the ferromagnetic structure and the layer type, rod type, and NaCl type antiferromagnetic structures, respectively.

$$\sum_{l=x,y,z} t_{ii+l}^{\gamma\gamma'}=\frac{3}{2}t_0\delta_{\gamma\gamma'}, \tag{6}$$

due to the cubic symmetry of the lattice and (2) the cubic symmetry of the spin structure, that is, spin F and G. Because of these two conditions, the orbital part in $H_{e\text{-}e}$ becomes diagonal and the A_{ij} term vanishes. On the other hand, in spin-A and -C phases, the orbital state is uniquely determined. In the spin-A phase, the orbital structure in the mean field theory is the orbital-C and -G phases with a $(\theta_A,\theta_B)=(\theta_A,-\theta_A)$-type orbital ordered state, where θ_A is determined by the equation $\theta_A=\cos^{-1}[2J_2/(5J_1-J_2)]$. It includes the $[(1/\sqrt{2})(3d_{3z^2-r^2}-3d_{x^2-y^2}),(1/\sqrt{2})(3d_{3z^2-r^2}+3d_{x^2-y^2})]$-type orbital ordered state at $J_2=0$ and the $(3d_{z^2-x^2},3d_{y^2-z^2})$-type ordered state at $J_2=J_1$.[7,24,25] The $(\theta_A,-\theta_A)$-type ordered state in the spin-A phase is consistent with the experimental results of the polarization dependence of the resonant x-ray scattering.[10,14] In the spin-C phase, the mean field solution is of orbital-G phase with a $(0,\pi)$-type state corresponding to the $(3d_{3z^2-r^2},3d_{x^2-y^2})$-type ordered state. In both cases, the spin structure breaks the cubic symmetry in the system and causes the anisotropic interaction between NN orbitals. This noticeable feature in the interplay between spin and orbital degrees clearly reflects on the dispersion relation of the orbital excitation, as will be discussed below.

We next study the orbital excitation in the orbital ordered states obtained in the mean field theory. The collective excitations in the orbital degree of freedom[26–28] are obtained by utilizing the conventional Holstein-Primakoff transformation. The spin structures are assumed to be frozen. The dispersion relation in the spin-F case is shown in Fig. 2 where the types of the orbital ordered state are chosen as $\theta_A=\pi n/6=\theta_B-\pi$. The face-centered cubic (fcc) lattice is adopted as a unit cell that includes two Mn ions. The analytic form of the dispersion relation and the eigenoperator are given by

$$\omega_k^{(\pm)}=3\sqrt{\Omega_A(\Omega_A\pm\Omega_B)}, \tag{7}$$

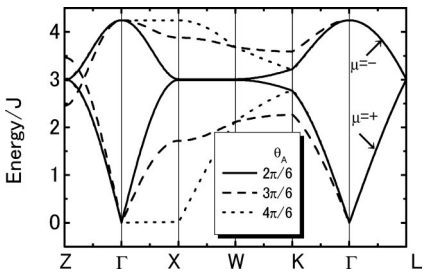

FIG. 2. The dispersion relation of the orbital wave in the spin-F case. The Brillouin zone for the face-centered cubic lattice is adopted. The orbital states for the two orbital sublattices are denoted by $(\theta_A, \theta_A+\pi)$. μ denotes the mode of the orbital wave.

with

$$\Omega_A = -2J_1\frac{1}{3}\sum_{l=x,y,z}(\tilde{\tau}_{ii+l})_{11}, \tag{8}$$

$$\Omega_B = 2J_1\frac{1}{3}\sum_{l=x,y,z}\cos(ak_l)(\tilde{\tau}_{ii+l})_{22}, \tag{9}$$

and

$$\alpha_k^{(\pm)} = \cosh\theta_k^{(\pm)}\frac{1}{\sqrt{2}}(a_k^{(A)} \pm a_k^{(B)}) + \sinh\theta_k^{(\pm)} \times \frac{1}{\sqrt{2}}(a_{-k}^{(A)\dagger} \pm a_{-k}^{(B)\dagger}), \tag{10}$$

with $2\theta_k^{(\pm)} = \tanh^{-1}[\pm\Omega_B/(2\Omega_A \pm \Omega_B)]$, respectively. $\tilde{\tau}_{ij}$ corresponds to τ_{ij} in the rotating frame. $a_k^{(A)}$ and $a_k^{(B)}$ are the Fourier transform of the Holstein-Primakoff boson for the two orbital sublattices defined in the rotating frame. The $(+)$ mode is the gapless mode and its eigenoperator includes the components $T_{Ax} - T_{Bx}$ and $T_{Ay} + T_{By}$. At the Γ point, the x component of the staggered orbital order parameter $\langle(\Sigma_{i\in A}T_{ix} - \Sigma_{i\in B}T_{ix})^2\rangle$ diverges since the orbital space is isotropic. As shown in Fig. 2, the stiffness of the orbital wave along the Γ-X direction becomes weak with increasing θ_A and it becomes flat at $\theta_A = (4\pi/6)(3d_{3x^2-r^2}, 3d_{y^2-z^2})$. It originates from $(\tilde{\tau}_{ii+x})_{22} = 0$ in Eq. (9), since the electron transfer between $3d_{y^2-z^2}$ orbitals along the x direction vanishes. The isotropic nature in the orbital space is seen by Fourier-transforming the Hamiltonian [Eq. (2)] as

$$H_{e\text{-}e} = -2J_1\sum_{\mathbf{k}}\left(\frac{3}{2} - \sum_{l=z,x}\hat{T}_l(\mathbf{k})\hat{\tau}_l(\mathbf{k})\hat{T}_l(\mathbf{k})\right), \tag{11}$$

in the spin-F case.[17] $\hat{T}_l(\mathbf{k})$ is the orbital pseudospin operator that diagonalizes the matrix τ_{ij} and

$$\hat{\tau}_l(\mathbf{k}) = 2[(c_x + c_y + c_z) \pm (c_x^2 + c_y^2 + c_z^2 - c_xc_y - c_yc_z - c_zc_x)^{1/2}], \tag{12}$$

where $+$ and $-$ are for $l = z$ and x, respectively, and $c_l = \cos(ak_l)$. At the Γ and R points, $\hat{\tau}_x = \hat{\tau}_z$, so that the orbital system becomes isotropic at these points.

The orbital excitation in the spin-A case is qualitatively different from that in the spin-F case as shown in Fig. 3. The unit cell with four Mn ions is adopted, so that there exist four modes. Two of them have the dispersion relations

$$\omega_k^{(+\pm)2} = \left(\Omega_{Axy} + \frac{\Omega_{Azz}}{2}\right)\left[(\Omega_{Axy} + \Omega_{Bxy}) + \frac{(\Omega_{Azz} \pm \Omega_{Bzz})}{2}\right], \tag{13}$$

and the other two $\omega^{(-\pm)}$ are given by replacing $(\Omega_{Axy} + \Omega_{Bxy})$ in Eq. (13) by $(\Omega_{Axy} - \Omega_{Bxy})$. Here,

$$\Omega_{Alm} = -2J_1\left(\frac{3}{4} + K_{lm}\right)(\tilde{\tau}_{lm})_{11} + 2J_2\left(\frac{1}{4} - K_{lm}\right) \times [(\tilde{\tau}_{lm})_{11} + 2(\tilde{M}_{lm})_1], \tag{14}$$

and

$$\Omega_{Blm} = \left[2J_1\left(\frac{3}{4} + K_{lm}\right) - 2J_2\left(\frac{1}{4} - K_{lm}\right)\right](\gamma_{lm})_{22}, \tag{15}$$

for $(lm) = (xy)$ or (zz). In these formulas, $A_{lm} = (1/2)\Sigma_{n=l,m}A_{ii+n}$ for $A = \tilde{\tau}$ and $\tilde{M}$ which corresponds to M in the rotating frame. $\gamma_{lm} = (1/2)\Sigma_{n=l,m}\tilde{\tau}_{ii+n}\cos(ak_n)$ and K_{lm} is the spin correlation function given by $K_{lm} = (1/2)\Sigma_{n=l,m}\langle(S_i)_z(S_{i+n})_z\rangle$. Among the four modes, the $(++)$ mode is the lowest one and its eigenoperator is expressed as

$$\alpha_k^{(++)} = \cosh\theta_k^{(++)}\frac{1}{2}(a_k^{(A1)} + a_k^{(A2)} + a_k^{(B1)} + a_k^{(B2)}) + \sinh\theta_k^{(++)}\frac{1}{2}(a_{-k}^{(A1)\dagger} + a_{-k}^{(A2)\dagger} + a_{-k}^{(B1)\dagger} + a_{-k}^{(B2)\dagger}), \tag{16}$$

where the superscripts $A(B)$ and 1 (2) imply the orbital and spin sublattices, respectively. This operator includes the components $T_{A1x} + T_{A2x} - T_{B1x} - T_{B2x}$ and $T_{A1y} + T_{A2y} + T_{B1y} + T_{B2y}$ and it corresponds to $(+)$ mode in the spin-F case. At the Γ point, the energy is obtained as

$$\omega_{k=\Gamma}^{(++)} = \frac{1}{2}\sqrt{(2\Omega_{Axy} + \Omega_{Azz})A^{(++)}}, \tag{17}$$

with

$$A^{(++)} = \sum_{(lm)=(xy),(zz)} z_{lm}\left\{\left[-2J_1\left(\frac{3}{4} + K_{lm}\right) + 2J_2\left(\frac{1}{4} - K_{lm}\right)\right][(\tilde{\tau}_{lm})_{11} - (\tilde{\tau}_{lm})_{22}] + 2J_2\left(\frac{1}{4} - K_{lm}\right)2(\tilde{M}_{lm})_1\right\}, \tag{18}$$

where $z_{xy} = 2$ and $z_{zz} = 1$. This mode has a gap in contrast with the spin-F case. The right hand side in Eq. (18) is represented by a product of the spin correlation function and the hopping integral, which has an anisotropic character. Therefore, the origin of the gap is attributed to the following facts: (1) The orbital space is anisotropic, i.e., $(\tilde{\tau})_{11} \neq (\tilde{\tau})_{22}$ and $A_{ij} \neq 0$, which originates from the anisotropic character of the hopping integral $t_{ij}^{\gamma\gamma'} \neq \delta_{\gamma\gamma'}t_0$. (2) The spin correlation

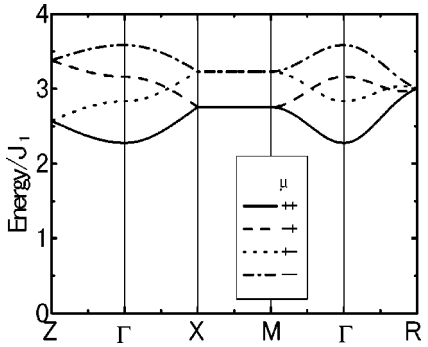

FIG. 3. The dispersion relation of the orbital wave in the spin-A case. The Brillouin zone for the tetragonal lattice is adopted. $J_2/J_1=0.5$, which corresponds to the orbital states $(\theta_A,-\theta_A)$ with $\theta_A=1.34$. μ denotes the mode of the orbital wave.

function in the xy plane and that in the z direction are different ($K_{xy}\neq K_{zz}$) in the spin-A case. The excitation with a gap is also obtained in the spin-C case. It is concluded that the anisotropic spin structure breaks the cubic symmetry and causes the gap in the orbital wave.

III. RESONANT INELASTIC X-RAY SCATTERING

In this section, we theoretically study RIXS as a probe to detect the orbital wave. The following two excitation processes are considered: the incident energy is tuned at (1) the Mn^{3+} L edge and (2) the Mn^{3+} K edge. The former and latter are termed L-edge and K-edge cases, respectively. We discuss qualitatively the general properties of the scattering due to the orbital wave, such as the excitation process, energy, and polarization dependences of the scattering cross section.

We first focus on the L-edge case. The excitation process is schematically shown in Fig. 4. The incident x ray excites an electron from the Mn $2p$ orbital to the unoccupied Mn $3d$ orbital, and then one of the $3d$ electrons fills the core hole by emitting an x ray. When the occupied orbitals are different between the initial and final states, the orbital excitation is brought about. This process is denoted by

$$|3d_\gamma^1\rangle+h\nu\rightarrow|3d_\gamma^1\underline{3d_{\bar{\gamma}}^1}\underline{2p}\rangle\rightarrow|3d_{\bar{\gamma}}^1\rangle+h\nu', \tag{19}$$

where $\underline{2p}$ implies that one hole occupies the Mn $2p$ orbital and γ ($\bar{\gamma}$) indicates the occupied (unoccupied) Mn $3d$ orbital in the initial state. It is noted that since the wavelength of the x ray for the L-edge case ($\sim$20 Å) is larger than the lattice constant ($\sim$4 Å) of the cubic unit cell, observed momentum of the orbital wave is limited in this case. The scattering cross section is calculated by the second order perturbation with respect to the electron-photon interaction. We consider the scattering where the momentum and energy of the incident (scattered) x ray are represented by $\mathbf{k}_{i(f)}$ and $\omega_{i(f)}$, respectively, and define $\mathbf{k}_{fi}=\mathbf{k}_f-\mathbf{k}_i$ and $\omega_{fi}=\omega_f-\omega_i$. The polarization vector of the incident (scattered) x ray are denoted by $\mathbf{e}_{i(f)}$. The most relevant term of the cross section is obtained as[29,20,21]

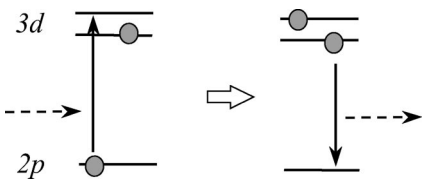

FIG. 4. The schematic picture of the orbital excitation processes in the L-edge case. The broken arrows indicate the incident and scattered x-rays.

$$\frac{d^2\sigma}{d\Omega d\omega_f}=\left(\frac{e^2}{mc^2}\right)^2\left(\frac{\omega_f}{\omega_i}\right)\sum_{\alpha G q\mu}(\mathbf{e}_i)_\alpha^2(\mathbf{e}_f)_\alpha^2\left|\frac{F_{\mu\alpha\mathbf{G}}(\mathbf{q})}{\Delta E}\right|^2 \times[\delta_{\mathbf{k}_{fi}+\mathbf{G}+\mathbf{q}}\delta(\omega_{fi}+\omega_q^{(\mu)})(1+n_q^{(\mu)}) +\delta_{\mathbf{k}_{fi}+\mathbf{G}-\mathbf{q}}\delta(\omega_{fi}-\omega_q^{(\mu)})n_q^{(\mu)}], \tag{20}$$

where $n_q^{(\mu)}$ is the number of the boson of mode μ and momentum $\mathbf{q}$, $\alpha=(x,y,z)$ and $\mathbf{G}$ is the reciprocal lattice vector. On resonance, the energy denominator ΔE, which indicates the difference between the energies for the initial and intermediate states, is assumed to be a constant of the order of a damping factor of the core hole Γ. In this formula, the generalized structure factor $F_{\mu\alpha\mathbf{G}}(\mathbf{q})$ is given by

$$F_{\mu\alpha\mathbf{G}}(\mathbf{q})=\frac{3}{2}\sum_\nu A_{\nu\gamma\alpha}^{(L)*}A_{\nu\gamma\alpha}^{(\underline{L})}[V_{\nu\mu}(\mathbf{q})+W_{\nu\mu}(\mathbf{q})]e^{i\mathbf{G}\cdot\mathbf{r}_\nu}. \tag{21}$$

$A_{l\gamma\alpha}^{(L)}$ is the coupling constant between the electronic current corresponding to the $2p\rightarrow3d$ transition at site l and the x ray divided by a factor $e/\sqrt{m}$. It is defined by

$$A_{l\gamma\alpha}^{(L)}=A_0\cos\left(\frac{\theta_\gamma}{2}+n_\alpha\frac{2\pi}{3}\right), \tag{22}$$

where A_0 is a constant, θ_γ is the angle in the orbital space for orbital γ and $(n_x,n_y,n_z)=(1,2,3)$. $V_{\nu\mu}(\mathbf{q})$ and $W_{\nu\mu}(\mathbf{q})$ in Eq. (21) are the coefficients in the Bogoliubov transformation, which connects the boson operator for the νth ion in the unit cell to that for the μth eigenmode as $a_q^{(\nu)}=\Sigma_\mu[V_{\nu\mu}(\mathbf{q})\alpha_q^{(\mu)}+W_{\nu\mu}(\mathbf{q})\alpha_{-q}^{(\mu)\dagger}]$.

We numerically calculate the square of the structure factor $I_L=|F_{\mu\alpha\mathbf{G}}(\mathbf{q})|^2/(3|A_0|^2/2)^2$. The results in the spin-F case with $(\theta_A,\theta_B)=(\pi/2,3\pi/2)$-type orbital ordered state and those in the spin-A case with $(\theta_A,\theta_B)=(1.34,-1.34)$-type state are presented in Figs. 5(a) and 5(b), respectively. We note the following characteristics in the scattering cross section: (1) The G dependence of the cross section is dominated by the factor $e^{i\mathbf{G}\cdot\mathbf{r}_\nu}$. In the spin-F case, the $+$ $(-)$ mode of the dispersion relation is observed only for $h+k+l=$ odd (even). Although this selection rule is broken in the spin-A case, the $(++(-))$ and $(-+(-))$ modes are mainly observed for $h+k=$ odd, $l=$ odd (even) and $h+k=$ even, $l=$ odd(even), respectively. (2) The $\mathbf{q}$ dependence of the scattering cross section is dominated by the factor $V_{\nu\mu}(\mathbf{q})+W_{\nu\mu}(\mathbf{q})$. In the spin-F case, the scattering intensity with $h+k+l=$ odd diverges at the Γ point due to this factor. (3) The polarization dependence is determined by the factor $A_{\nu\gamma\alpha}^{(L)*}A_{\nu\gamma\alpha}^{(\underline{L})}$, which is proportional to $\sin(\theta_\gamma+n_\alpha4\pi/3)$. Due to this factor, the scattering cross section for $\alpha=z$ is larger than that for $\alpha=x(y)$.

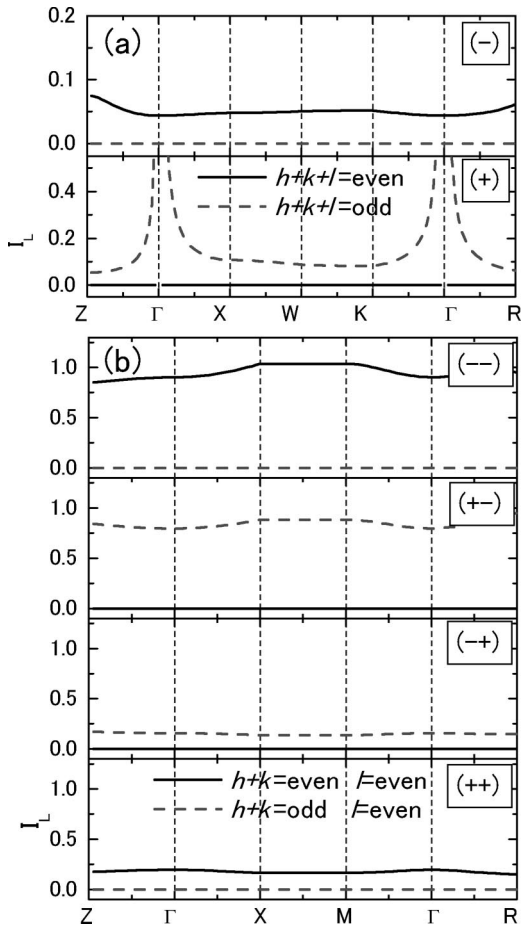

FIG. 5. The square of the structure factor for the orbital wave in the *L*-edge case. The polarization is parallel to the *x* direction. (a) spin-F case with $(\pi/2,\pi/2+\pi)$-type orbital ordered state. Solid and dashed lines show the squares of the structure factor for $h+k+l=$even and odd, respectively. (b) Spin-A case with $(\theta_A,-\theta_A)$-type orbital ordered state with $\theta_A=1.34$ $(J_2/J_1=0.5)$. Solid and dashed lines show the squares of the structure factor for $h+k=$even, $l=$even, and $h+k=$odd, $l=$even, respectively. $(\pm)$ and $(\pm\pm)$ indicate the modes of the orbital wave.

In the *K*-edge case of RIXS, we propose the following two excitation processes of the orbital wave. The schematic pictures of the processes are shown in Fig. 6. (a) The incident x ray excites an electron from the Mn $1s$ orbital to the Mn $4p$ orbital. In the intermediate state, the $3d$ electron is excited from the occupied orbital to the unoccupied one through the Coulomb interaction between $3d$ and $4p$ electrons. Finally, the $4p$ electron fills the core hole by emitting x ray. This process is denoted by

$$|3d_\gamma^1\rangle+h\nu\rightarrow|3d_\gamma^1 4p^1\underline{1s}\rangle\rightarrow|3d_{\bar{\gamma}}^1 4p^1\underline{1s}\rangle\rightarrow|3d_{\bar{\gamma}}^1\rangle+h\nu'. \tag{23}$$

The one-orbital wave excitation occurs at the site where the x ray is absorbed. (b) In the intermediate state in the scattering, one hole is created in the Mn $1s$ orbital. In order to screen the core hole potential, an electron comes from one of the NN O $2p$ orbitals to the Mn site. Due to the hybridization between the O $2p$ and Mn $3d$ orbitals, this state strongly mixes with the state where the e_g orbitals in one of the NN Mn sites (j site) are empty. When the $4p$ electron fills the $1s$ orbital by emitting an x ray, one of the $3d$ electrons in the i site comes back to the j site. This process is denoted by

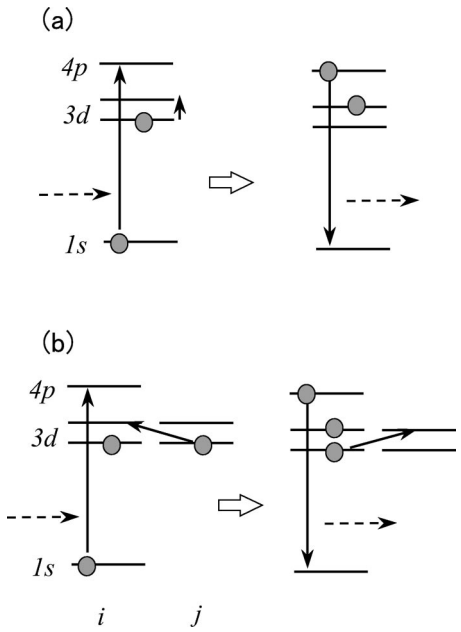

FIG. 6. The schematic picture of the orbital excitation processes in the *K*-edge case. j denotes one of the nearest neighboring sites of i. The broken arrows indicate the incident and scattered x rays.

$$|3d_{i\gamma_i}^1 3d_{j\gamma_j}^1\rangle+h\nu\rightarrow|3d_{i\gamma_i}^1 3d_{i\gamma_i'}^1\underline{1s_i}4p_i^1\rangle \rightarrow|3d_{i\gamma_i''}^1 3d_{j\gamma_j'}^1\rangle+h\nu', \tag{24}$$

where O $2p$ states are integrated out. Both one- and two-orbital wave excitations occur in i and j sites. In the several transition metal oxides, the final state of the x-ray absorption spectroscopy (XAS), which corresponds to the intermediate state of RIXS with the lowest energy, is assigned as the so-called well screened state $|3d^2 4p^1\underline{1s}\,\underline{L}\rangle$, which mixes with the state $|3d^1 4p^1\underline{1s}\rangle$.[23,30,31,13] Here, $\underline{L}$ implies that one hole occupies the NN O $2p$ orbital. Therefore, both excitation processes, that is, (a) and (b), are the main processes of x-ray scattering by the orbital wave in the *K*-edge case. In the case of the manganites, process (b) occurs more easily than in cuprates and nickelates, because the effective intrasite Coulomb interaction between $3d$ electrons is smaller in manganites.[32]

The scattering cross section in process (a) is given by the same form with Eq. (20), where the most relevant term of the form factor is obtained as

$$F_{\mu\alpha\mathbf{G}}(\mathbf{q})=2|A^{(K)}|^2\sum_\nu \frac{\bar{V}_\nu^{\gamma\gamma\alpha\alpha}}{\Delta\varepsilon_\nu^{\gamma\alpha}}[V_{\nu\mu}(\mathbf{q})+W_{\nu\mu}(\mathbf{q})]e^{i\mathbf{G}\cdot\mathbf{r}_\nu}, \tag{25}$$

where $A^{(K)}$ is the coupling constant between the electronic current corresponding to the $1\underline{s}\rightarrow 4p$ transition and the x ray divided by a factor $e/\sqrt{m}$.[13] $V_\nu^{\gamma\gamma\alpha\alpha}$ is the off-diagonal matrix element of the Coulomb interaction between Mn $3d$ and $4p$ electrons defined by

$$V_{\nu}^{\bar{\gamma}\gamma\alpha\alpha}=e^2\int d\mathbf{r}_1 d\mathbf{r}_2 \frac{\phi_{d_{\bar{\gamma}}}(\mathbf{r}_1)^*\phi_{d_\gamma}(\mathbf{r}_1)\phi_{p_\alpha}(\mathbf{r}_2)^*\phi_{p_\alpha}(\mathbf{r}_2)}{|\mathbf{r}_1-\mathbf{r}_2|}$$
$$=\frac{4}{35}F^{(2)}\sin\left(\theta_\gamma+\frac{n_\alpha 4\pi}{3}\right), \tag{26}$$

where ϕ_{d_γ} (ϕ_{p_α}) is the atomic wave function of the $3d$ ($4p$) electron with orbital γ (α) and $F^{(2)}$ is the Slater integral between $3d$ and $4p$ electrons. $\Delta\varepsilon_\nu^{\gamma\alpha}$ indicates difference between the energy for the intermediate state with the lowest excitation energy and that for the state $|3d_{\gamma}^{\bar{1}}4p_{\alpha}^{1}\underline{1s}\rangle$. It is clear from Eqs. (21) and (25) that the G and q dependences of the cross section in this case are the same as those in the L-edge case. Although the polarization dependence of the scattering factor is provided by the two factors $V_\nu^{\bar{\gamma}\gamma\alpha\alpha}$ and $\Delta\varepsilon_\nu^{\gamma\alpha}$ in Eq. (25), the former is a dominant term and is proportional to $\sin(\theta_\gamma+n_\alpha 4\pi/3)$ as well as $A_{\nu\gamma\alpha}^{(L)*}A_{\nu\bar{\gamma}\alpha}^{(\underline{L})}$ in Eq. (21).

On the other hand, the most relevant term of the scattering cross section in process (b) with the one-orbital wave excitation is given by Eq. (20) with

$$F_{\mu\alpha\mathbf{G}}(\mathbf{q})=2|A^{(K)}|^2\sum_{\nu\nu'}e^{i\mathbf{G}\cdot\mathbf{r}_\nu}\left(\frac{3}{4}+\langle\mathbf{S}_\nu\cdot\mathbf{S}_{\nu'}\rangle\right)$$
$$\times\left\{-[V_{\nu\mu}(\mathbf{q})+W_{\nu\mu}(\mathbf{q})]\frac{t_{\nu\nu'}^{\gamma\gamma}t_{\nu\nu'}^{\bar{\gamma}\gamma}}{\delta\varepsilon_\nu^{\gamma\alpha}\delta\varepsilon_\nu^{\bar{\gamma}\alpha}}+[V_{\nu'\mu}(\mathbf{q})\right.$$
$$\left.+W_{\nu'\mu}(\mathbf{q})]\frac{t_{\nu\nu'}^{\bar{\gamma}\gamma}t_{\nu\nu'}^{\bar{\gamma}\gamma}}{\delta\varepsilon_\nu^{\gamma\alpha 2}}e^{i\mathbf{q}\cdot(\mathbf{r}_\nu-\mathbf{r}_{\nu'})}\right\}, \tag{27}$$

where ν and ν' indicate the site where the x ray is absorbed and its NN site, respectively. $\delta\varepsilon_\nu^{\gamma\alpha}$ is difference between the energy for the well screened state $|3d_{\nu\gamma}^{1}3d_{\nu\bar{\gamma}}^{1}\underline{1s_\nu}4p_{\nu\alpha}^{1}\underline{L}\rangle$ and that for the poorly screened one $|3d_{\nu\gamma}^{1}\underline{1s_\nu}4p_{\nu\alpha}^{1}\rangle$. The two terms in the curly bracket in Eq. (27) correspond to the orbital excitations at sites ν and ν', respectively.

We present the numerical results of the square of the structure factor in case (b), $I_K=|F_{\mu\alpha}(\mathbf{q})/\Delta E|^2/(2|A^{(K)}|^2t_0^{-1})^2$, in Figs. 7(a) and 7(b), where the spin and orbital states are chosen to be the same with those in Figs. 5(a) and 5(b), respectively. In comparison with the L-edge case, we note the following characteristics: (1) Even in the spin-F case, the selection rule between the modes of the orbital wave and $\mathbf{G}$ is broken. (2) The $\mathbf{q}$ dependence of the cross section is caused by the factor $e^{i\mathbf{q}\cdot(\mathbf{r}_\nu-\mathbf{r}_{\nu'})}$ in Eq. (27) and is more remarkable than that in the L-edge case. In particular, the scattering cross section is zero at the Γ-point in spin-F case [Fig. 7(a)]. This is attributed to the relations of the hopping integral: $\Sigma_\delta t_{\nu\nu+\delta}^{\gamma\gamma}t_{\nu\nu+\delta}^{\bar{\gamma}\gamma}=0$ and $\Sigma_\delta t_{\nu\nu+\delta}^{\bar{\gamma}\gamma}t_{\nu\nu+\delta}^{\gamma\gamma}=0$. (3) The polarization dependence of the intensity is caused by $\delta\varepsilon_\nu^{\gamma\alpha}$ and is weaker than that in the L-edge case.

IV. SUMMARY AND DISCUSSION

We study the orbital excitation in the orbital ordered manganites and reveal the correlation between the spin structure and the dispersion relation of the orbital wave. The gap in the orbital wave is caused by an anisotropic spin structure such as the spin-A structure. On the other hand, the orbital wave is gapless in the spin-F and paramagnetic spin structures where the cubic symmetry is preserved. In the calculation in Sec. II, the spin degree of freedom is assumed to be frozen. On the contrary, in Refs. 26 and 27, roles of the spin fluctuations on the orbital excitation were investigated in the model Hamiltonian with $S=1/2$ and no Hund coupling between e_g electrons. It was shown that the spin fluctuation originating from the anisotropic exchange interaction breaks the cubic symmetry even in the ferromagnetic phase and affects the gap and the dispersion relation of the orbital wave. However, in the manganites, the effects of the spin fluctuation may be neglected, because the magnitude of spin in a Mn^{3+} ion is $S=2$ due to the strong Hund coupling, and the almost full magnetic moment is experimentally confirmed at low temperatures.[3]

$LaMnO_3$ below the Néel temperature is one of the candidates for the system where the excitation with a gap exists.

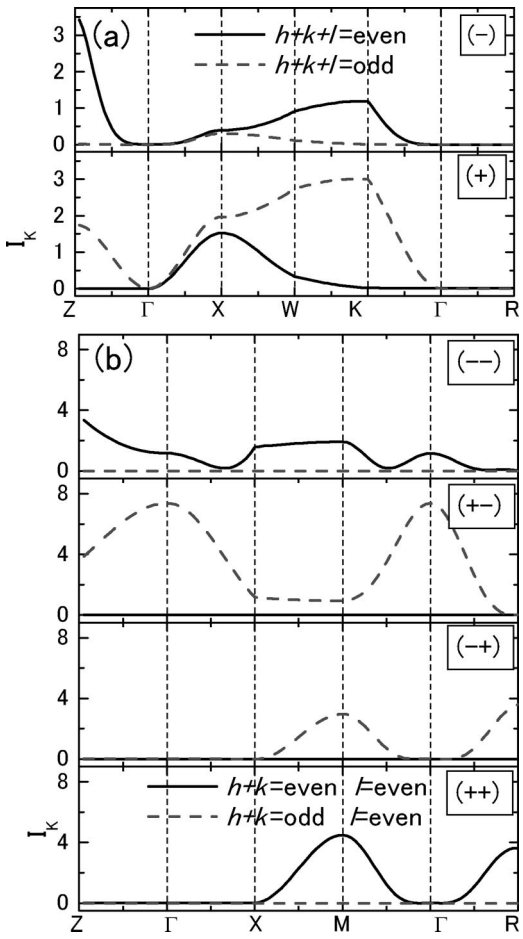

FIG. 7. The square of the structure factor for the orbital wave in the K-edge case [process (b)]. The polarization is parallel to the x direction. (a) Spin-F case with $(\pi/2,\pi/2+\pi)$-type orbital ordered state. Solid and dashed lines show the squares of the structure factor for $h+k+l=$ even and odd, respectively. (b) Spin-A case with $(\theta_A,-\theta_A)$-type orbital ordered state with $\theta_A=1.34$ ($J_2/J_1=0.5$). Solid and dashed lines show the squares of the structure factor for $h+k=$ even, $l=$ even and $h+k=$ odd, $l=$ even, respectively. $(\pm)$ and $(\pm\pm)$ indicate the modes of the orbital wave.

The magnitude of the gap in the present mechanism is of the order of $zt_0^2/U \sim 0.1$ eV, where z is the number of the NN Mn ions. The Jahn-Teller type distortion in a MnO_6 octahedron also contributes to the gap of the orbital excitation. Since the gap is larger than the band width of the spin wave [~ 0.04 eV (Refs. 16 and 33)] and that of the Jahn-Teller mode of phonon [~ 0.05 eV (Refs. 34 and 35)], the couplings between the orbital wave and these excitations are weak. In the spin-F case, the orbital excitation becomes gapless and the low-lying excitation affects the thermodynamic and electrical transport. The specific heat, being proportional to T^3, is caused by the linear dispersion relation and is distinguishable from the $T^{3/2}$ component caused by the ferromagnetic spin wave. One possible candidate, where the gapless excitation is anticipated, is the ferromagnetic insulating phase in lightly doped manganites. In $La_{0.88}Sr_{0.12}MnO_3$, the orbital ordering is confirmed by the resonant x-ray scattering below $T_{OO} = 145$ K where the static Jahn-Teller distortion is almost quenched.[11] The low-lying excitation is expected to be observed without disturbance of the static lattice distortion.

In the spin canted phase, the gap gradually decreases with decreasing canting angle. The magnitude of the gap is also changed by applying a magnetic field in the spin-A state. With increasing field, the gap is gradually reduced and the excitation becomes gapless at the transition from the canted spin-A state to the spin-F one.

The energy resolution of RIXS to detect the dispersion relation of the orbital wave is required to be of the order of the interaction between the NN orbital pseudospins, which is estimated as $zt_0^2/U \sim 0.1$ eV. It will be possible to realize the resolution in the recent RIXS experiments.

ACKNOWLEDGMENTS

The authors would like to thank Y. Endoh, Y. Murakami, and J. Mizuki for their valuable comments on the experimental setup. We are also indebted to M. Kaji and S. Okamoto for their helpful discussions and calculations. This work was supported by Priority Areas Grants from the Ministry of Education, Science and Culture of Japan, CREST (Core Research for Evolutional Science and Technology Corporation) Japan, and NEDO Japan. Part of the numerical calculation was performed in the HITACS-3800/380 supercomputing facilities in Institute for Materials Research, Tohoku University.

[1] K. Chahara, T. Ohono, M. Kasai, Y. Kanke, and Y. Kozono, Appl. Phys. Lett. **62**, 780 (1993).
[2] R. von Helmolt, J. Wecker, B. Holzapfel, L. Schultz, and K. Samwer, Phys. Rev. Lett. **71**, 2331 (1993).
[3] Y. Tokura, A. Urushibara, Y. Moritomo, T. Arima, A. Asamitsu, G. Kido, and N. Furukawa, J. Phys. Soc. Jpn. **63**, 3931 (1994).
[4] S. Jin, T. H. Tiefel, M. McCormack, R. A. Fastnacht, R. Ramesh, and L. H. Chen, Science **264**, 413 (1994).
[5] J. B. Goodenough, Phys. Rev. **100**, 564 (1955).
[6] J. Kanamori, J. Phys. Chem. Solids **10**, 87 (1959).
[7] K. I. Kugel and D. I. Khomskii, Zh. Éksp. Teor. Fiz., Pis'ma Red. **15**, 629 (1972) [JETP Lett. **15**, 446 (1972)].
[8] Y. Ito, and J. Akimitsu, J. Phys. Soc. Jpn. **40**, 1333 (1976).
[9] Y. Murakami, H. Kawada, H. Kawata, M. Tanaka, T. Arima, H. Moritomo, and Y. Tokura, Phys. Rev. Lett. **80**, 1932 (1998).
[10] Y. Murakami, J. P. Hill, D. Gibbs, M. Blume, I. Koyama, M. Tanaka, H. Kawata, T. Arima, T. Tokura, K. Hirota, and Y. Endoh, Phys. Rev. Lett. **81**, 582 (1998).
[11] Y. Endoh, K. Hirota, S. Ishihara, S. Okamoto, Y. Murakami, A. Nishizawa, T. Fukuda, H. Kimura, N. Nojiri, K. Kaneko, and S. Maekawa, Phys. Rev. Lett. **82**, 4328 (1999).
[12] K. Nakamura, T. Arima, A. Nakazawa, Y. Wakabayashi, and Y. Murakami, Phys. Rev. B **60**, 2425 (1999).
[13] S. Ishihara, and S. Maekawa, Phys. Rev. Lett. **80**, 3799 (1998).
[14] S. Ishihara, and S. Maekawa, Phys. Rev. B **58**, 13 442 (1998).
[15] M. Cyrot, and C. Lyon-Caen, J. Phys. (Paris) **36**, 253 (1975). The collective excitation in the model where the orbital space is anisotropic was studied by A. G. Komarov, L. I. Korovin, and E. K. Kudinov, Fiz. Tverd. Tela (Leningrad) **17**, 2315 (1975) [Sov. Phys. Solid State **17**, 1531 (1975)].
[16] S. Ishihara, J. Inoue, and S. Maekawa, Physica C **263**, 130 (1996); Phys. Rev. B **55**, 8280 (1997).
[17] S. Ishihara, M. Yamanaka, and N. Nagaosa, Phys. Rev. B **56**, 686 (1997).
[18] J. van den Brink, W. Sekelenburg, D. I. Kohmskii, G. A. Sawatzky, and K. I. Kugel, Phys. Rev. B **58**, 10 276 (1998).
[19] J. Inoue, S. Okamoto, S. Ishihara, W. Koshibae, Y. Kawamura, and S. Maekawa, Physica B **237-238**, 51 (1997).
[20] P. M. Platzman, and E. D. Isaacs, Phys. Rev. B **57**, 11 107 (1998).
[21] *Raman Emission by X-ray Scattering*, edited by D. L. Ederer and J. H. McGuire (World Scientific, Singapore, 1996).
[22] P. Kuiper, J. -H. Guo, C. Sathel, L. -C. Duda, J. Nordgren, J. J. M. Pothuizen, F. M. F. de Groot, and G. A. Sawatzky, Phys. Rev. Lett. **80**, 5204 (1998).
[23] J. P. Hill, C. -C. Kao, W. A. L. Caliebe, M. Matsubara, A. Kotani, J. L. Peng, and R. L. Greene, Phys. Rev. Lett. **80**, 4967 (1998).
[24] R. Maezono, S. Ishihara, and N. Nagaosa, Phys. Rev. B **57**, R13 993 (1998).
[25] R. Shiina, T. Nishitani, and H. Shiba, J. Phys. Soc. Jpn. **66**, 3159 (1997).
[26] G. Khaliullin and V. Oudovenko, Phys. Rev. B **56**, R14 243 (1998).
[27] L. F. Feiner, A. M. Oles, and J. Zaanen, J. Phys.: Condens. Matter **10**, L555 (1998).
[28] J. van den Brink, P. Horsch, F. Mack, and A. M. Oles, Phys. Rev. B **59**, 6795 (1999).
[29] M. Blume, J. Appl. Phys. **57**, 3615 (1985).
[30] J. M. Tranquada, S. M. Heald, W. Kunnmann, A. R. Moodenbaugh, S. L. Qiu, Y. Xu, and P. K. Davies, Phys. Rev. B **44**, 5176 (1991).
[31] A. Sahiner, M. Croft, S. Guha, I. Perez, Z. Zhang, M. Greenblatt, P. A. Metcalf, H. Jahns, and G. Liang, Phys. Rev. B **51**, 5879 (1995).
[32] T. Arima, Y. Tokura, and J. B. Torrance, Phys. Rev. B **48**, 17 006 (1993); A. E. Bocquet, T. Mizokawa, K. Morikawa, A. Fujimori,

S. R. Barman, K. Maiti, D. D. Sarma, Y. Tokura, and M. Onoda, *ibid.* **53**, 1161 (1996).
[33] K. Hirota, N. Kaneko, A. Nishizawa, and Y. Endoh, J. Phys. Soc. Jpn. **65**, 3736 (1996).
[34] K. Yamamoto, Masters thesis, University of Tokyo, 1996.
[35] M. N. Iliev, M. V. Abrashev, H. -G. Lee, V. N. Popov, Y. Y. Sun, C. Thomsen, R. L. Meng, and C. W. Chu, Phys. Rev. B **57**, 2872 (1998).